

<https://doi.org/10.1038/s44304-024-00018-7>

Seismic signature of an extreme hydro-meteorological event in Italy

**Velio Covello¹, Mauro Palo², Elisa Adirosi³ & Matteo Picozzi^{2,4}**

Flash floods are a major threat for Mediterranean countries and their frequency is expected to increase in the next years due to the climatic change. Civil protection agencies are called to deal with increasing hydrological risk, but existing hydro-meteorological monitoring networks might not be enough for detecting, tracking, and characterizing rapidly evolving floods produced by severe convective storms. Nowadays, hydro-meteorological information in several watersheds particularly in small and mid-size in orographically complex regions or in third-world countries, is still not available or insufficient. To improve our observational capability of these events, we propose to exploit the seismic recordings, which act as opportunistic signals and can complement well-established procedures to early detect the occurrence of flash floods at regional scale. Here, we investigate the hydro-meteorological event that hit central Italy in September 2022 and resulted in a devastating flash flood. We compare seismic data from a national monitoring network with raingauges and hydrometer data. Our evidence suggests that the main stages of the hydro-meteorological events can be tracked by the spatio-temporal evolution of the seismic noise confirming the capability of this multi-sensor approach in detecting and characterizing such kind of events.

Flash floods are triggered by high-intensity and short-duration rainfalls and represent a major hazard for small river basins^{1,2}. Given the heavy rainfall in a short period of time and the following rapid concentration of the runoff, flash floods populate the upper tail of the flood frequency distribution in small- to medium-size catchments (10^3 – 10^4 km 2), posing at high-risk large communities and infrastructures. The flash floods risk is exacerbated by the increase in frequency of extreme meteorological events. This increase is nowadays more and more imputed by the scientific community to the consequences of the climate changes; for instance, according to climate model projections, the annual damage caused by flooding in the United Kingdom is expected to increase by more than one fifth over the next century if the COP26 and Net Zero promises are not collectively met³.

The Mediterranean region is particularly exposed to the consequences of climate change, and despite the foreseen overall drying, extreme precipitation events are expected to increase⁴. It seems reasonable that even the population exposure to floods is expected to increase at regional scales given the population growth that the Mediterranean basin is experiencing.

Italy is exposed to high hydrological risk. A consistent number of flood events occurred there in the recent years, such as: the one occurred in Liguria on October 2021⁵; those in the island of Ischia on October 2009⁶ and in

November 2022; the recent flood that hit the Marche region on the 15 September 2022⁷, which is the target of this work. A detailed list of floods occurred in Italy and all over the word can be found at FloodList (<https://floodlist.com/>).

Italy has an advanced multi-parametric real-time monitoring system (i.e., raingauges, hydrometers) to detect and monitor hydro-meteorological events, and the national civil protection agency has at its disposal even ground-based weather radars and satellite-borne active and passive sensors. However, it is worth noting that the effects and damages caused by some events (such as the one occurred on the 15 September 2022) highlights as dealing with extreme large-scale floods calls for a paradigm change in monitoring.

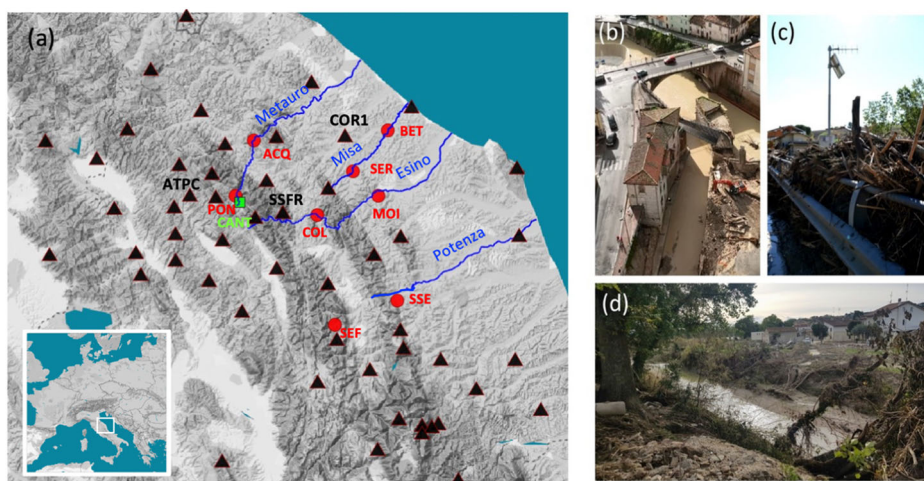
Raingauges are the most widely used devices to monitor local precipitation data, yielding accurate and direct measurement of rain accumulation (in mm). These devices collect data for a specific installation site, but due to the high temporal and spatial variability of precipitation, the recorded data at one site result often not correlated with the precipitation at surrounding areas. To improve the spatial accuracy of rainfall estimates from rain gauges, it might be convenient to consider a network of rain gauges, but even this solution turns out to be inefficient due to the spatially

¹National Research Council of Italy, Research Institute for Geo-Hydrological Protection, (CNR-IRPI), Padova, Italy. ²Physics Department “Ettore Pancini”, University of Naples Federico II, Naples, Italy. ³National Research Council of Italy, Institute of Atmospheric Sciences and Climate (CNR-ISAC), Rome, Italy. ⁴National Institute of Oceanography and Applied Geophysics – OGS, Trieste, Italy. e-mail: matteo.picozzi@unina.it; mpicozzi@ogs.it

Table 1 | Density of the seismic networks used for the detection and tracking of meteorological and/or debris flow events in some recent publications

| Author | Number of used seismometers | Target area |
|--------------------------------------|-----------------------------|---|
| Abancò et al. ²⁴ | 2 | Rebaixader, Central Pyrenees, Spain |
| Coviello et al. ^{21,25} | 3 | Cenischia valley and Gadria–Strimm basins, Italian Alps |
| Walter et al. ²⁶ | 10 | Illgraben, Switzerland |
| Cook et al. ³⁰ | 76 | Uttarakhand, northern India |
| Rindraharisaona et al. ²⁸ | 3 | La Reunion Island |
| Bakker et al. ²⁷ | 3 | Galabre catchment, France |
| Diaz et al. ²⁹ | 140 | Cerdanya basin, Eastern Pyrenees, Spain |
| Dietze et al. ¹⁰ | 1 | Ahrtal, Germany |

Fig. 1 | Distribution of rivers, stations, and example of damages. The area hit by the Marche hydrological crisis occurred between 12:00 and 20:00 UTC of the 15 September 2022. **a** Distribution of seismic stations (black triangles). Please note, those discussed in the main text and shown in Fig. 2 are highlighted by the IV seismic network code: COR1, ATPC, SSFR. A complete map of the seismic stations can be found in Fig. S2. Hydrometers discussed in the main text (red circles): Pontedazzo, PON, Bettolle, BET, Moie, MOI, and S. Severino, SSE, Acqualagna, ACQ, Serra dei conti, SER, Colleponi, COL, Sefro, SEF. The green square marks the position of the Cantiano (CANT) rain gauge mentioned in the text. From **b** to **d**: examples of damages at villages between the Metauro and Misa rivers.



inhomogeneous rain gauges network density⁸. On the other hand, weather radars can provide spatial features of precipitation with high spatial (less than 1 km, although not uniform) and temporal resolution (5–10 min). However, they only provide indirect measurements of precipitation, which requires appropriate retrieval algorithms and can be affected by many errors⁹. The latter issue is particularly relevant in complex orographic areas, where the radar beam can be completely or partially blocked by natural obstacles. Even hydrometric networks provide useful information but are prone to problems. It seems indeed that hydrometers are not fully adequate to monitor the evolution of flash floods, given: (i) the low temporal resolution of the measurement, (ii) the exposure to damage by water discharge, coarse sediment and large wood transport, (iii) the lack of information beyond stage height, and (iv) malfunctioning due to erosion/deposition processes^{10–12}. For instance, most of the hydrometers in Italy sample water level once in 30 min, which seems insufficient to characterize rapidly evolving floods featuring short-duration pulses. It then becomes clear that, although the damage potential of flash floods is well known, the capability to monitor them can be limited due to the quantity and type of instruments normally adopted for monitoring. This can be a relevant limitation for understanding the hydro-meteorological processes that control flash floods. In this concern, there is the urgency to make the monitoring system more efficient and reliable, even by integrating opportunistic information provided by different sensors.

Recent studies have explored the possibility to detect and monitor meteorological and/or debris flow events by seismic noise (Table 1). Different structural and environmental factors are responsible for the temporal and spatial variation of seismic noise¹³. Non-tectonic seismic sources such as landslides, debris flows, dam collapses, floods, and avalanches generate seismic signals that are considered as “exotic” sources of noise when the

objective is to perform a classical seismological analysis. Building upon a pioneering experiment carried out in the early 90s¹⁴, a growing number of studies dealing with the monitoring of river networks during monsoons¹⁵, typhoons¹⁶, and controlled floods¹⁷ are nowadays relying on seismometers placed near torrents. Separating the contribution of various “exotic” seismic sources – including precipitation, bedload transport, and flow turbulence – would allow to characterize different processes with a single sensor at very high temporal resolution.

Fluvial seismology has already shown that important characteristics about river flow processes, such as bedload transport and turbulence, are encoded in ground vibrations¹⁸. Worth to mention, during the last twenty years, the Italian seismological community made great efforts in establishing dense seismic networks at national scale, standardizing formats for data transmission and archiving, and creating open data repositories for sharing real-time and archived data streams (e.g., the Observatories and Research Facilities for European Seismology European Integrated Data Archive, <https://www.orfeus-eu.org/data/eida/>). Such infrastructure and methodological developments open new scientific avenues, including the upscaling of fluvial seismology from single rivers to watersheds, which would be precious during large-scale flash floods.

In this work, we study the spatio-temporal evolution of seismic noise recorded before, during and after the 15 September 2022 event that occurred in the Marche Region in Italy. Specifically, we evaluate the recordings of 54 three-component broad-band stations of the permanent Italian seismic monitoring network surrounding the target area with an inter-station distance in the order of 10 km (Fig. 1). Our aim is to verify whether, as suggested by previous studies¹⁰, seismic noise amplitude changes in time according to the evolution of the hydro-meteorological event. If we were able to observe seismic noise being tied to hydro-meteorological

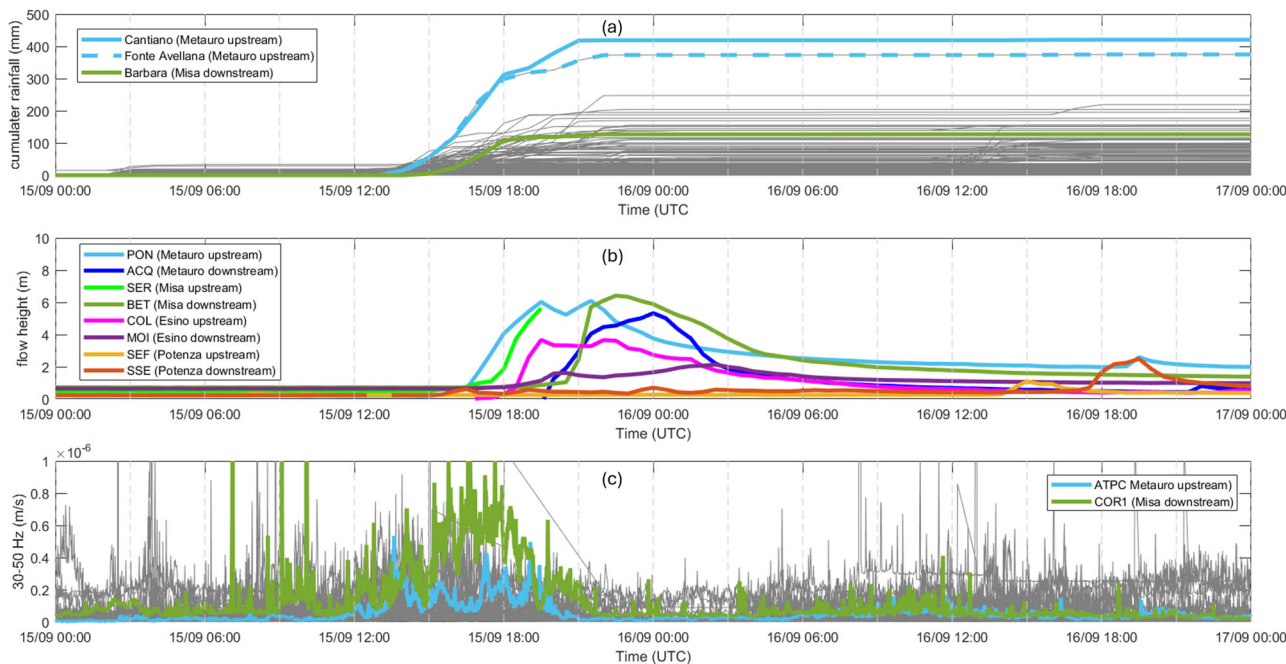


Fig. 2 | Temporal evolution of raingauges, hydrometer, and seismic data. **a** Time series of the cumulated rainfall (mm) between the 15 and the 17 September 2022 obtained from all raingauges considered in this study (gray lines). Please note that the distribution of raingauges is shown in Fig. S1. The light blue lines represent the cumulated rainfall registered at Cantiano and Fonte Avellana stations, which are 6.9 km apart and are located upstream of Metauro river; the dark green line shows

the same quantity recorded at the Barbara station in the lower part of the Misa river. **b** Time series of the flow heights (in meters) registered between the 15 and 17 September 2022 by eight hydrometers located in the river basin involved in the event (whose location is shown in Fig. 1a). **c** Envelopes on the seismic signals for the stations shown in Fig. 1a (gray lines) and with the stations COR1 and ATPC highlighted.

characteristics, in the future civil protection agencies could integrate seismic noise information as opportunistic data in their emergency protocols. Therefore, in this work, we analyze seismic data collected during the days 15 and 16 September 2022, and we compare the spatio-temporal evolution of seismic noise amplitudes with both the precipitation and the river water level collected by conventional networked devices. Our results show a good spatial match between high seismic amplitudes and the principal rivers of the area, where indeed most damaged villages are located and indicate eventually that the analysis of the seismic noise recorded by dense, regional seismic networks can provide powerful information on the spatio-temporal evolution of the flood that can efficiently complement hydrometric data.

September 2022. In the final part of that day, the system progressively moved towards the coast, gradually weakening in its intensity. At the same time, another thunderstorm system developed in the southern part of the region persisting for a more limited period, with intense phenomena but with considerably lower accumulations. To highlight the strength of the 15 September 2022 hydro-meteorological event, which leads us to define it as an extreme one, we recall that its total rainfall accumulation (437 mm) was more than the half of the total accumulation value for the Marche region over an entire year (i.e., the mean annual precipitation over the 1981–2010 period is 803.6 mm, <https://www.reterurale.it/flex/cm/pages/ServeBLOB.php/L/IT/IDPagina/16319>).

The 15 and the 16 September 2022 flash flood in Italy

The flash flood that hit the Marche region (Central Italy) between the 15 and the 16 September 2022 (Fig. 1) cumulated a rainfall peak of 437 mm in <12 h (measured at the Cantiano rain gauge), which according to historical catalogs of rainfall events corresponded to an event with a return period exceeding 500 years¹⁹. The 15 September 2022 rainfall triggered 1687 landslides in an area of 550 km² affected by the highest rainfall intensity²⁰ and led to 12 fatalities and severe damages to transport, infrastructures, and buildings, especially in the Misa basin (Fig. 1). Such an exceptionally severe event occurred at the end of a climatic anomaly of prolonged drought and warm conditions over Europe and the Mediterranean region. The 15 September 2022 event resulted from the unlucky combination of a deep trough over Scandinavia, a secondary lower one over the Iberian Peninsula and a high pressure on North Africa, which produced convective systems on the Tyrrhenian side. The slow movement of such baric structures determined the stationarity of its western flow in which these convective structures were developing. Consequently, they continued to affect the same area for several hours, resulting in very high accumulations. In the early afternoon of the 15 September 2022, storm cells developed on the Apennines side in the mountain part of Marche region, generating intense, localized, and stationary phenomena. Of note, there was a low-level hydrogeological and meteorological warning for thunderstorms and strong winds for the 15

Results

Temporal evolution of raingauges, hydrometer, and seismic data

Cumulated rainfall time series of raingauges in the Marche and Umbria regions (Figs. 2a and S1) provide a clear picture of the temporal evolution of the meteorological event that occurred between the 15 and 16 September 2022. A couple of raingauges (i.e., Cantiano and Fonte Avellana stations) that are in the upper part of the Metauro river basin and are 6.9 km apart each other (light blue lines in Fig. 2a), recorded between 12.00 and 20.00 UTC of the 15 September 2022 a huge amount of precipitation, reaching a cumulative value of about 400 mm. This value is significantly larger than the cumulative precipitation measured during the crisis at any other station in the region.

The temporal evolution of eight available hydrometers located in the basin of the rivers involved in the event provides useful information, as well (Fig. 2b). Metauro and Misa rivers were largely hit by the event. Accordingly, the stations at Pontedazzo (PON) - located on the upper part of the Metauro river - recorded over 6 m of flow height, while the downstream station (Acqualagna, ACQ) recorded up to 5 m of flow height. Unfortunately, the cable of Misa upper stream hydrometer (Serra dei Conti, SER) was damaged by the flood and stopped recording at 19:30 UTC of the 15 September (see supplemental material). As previously discussed, the damage of hydrometers and the following loss of information represents a serious drawback

for the monitoring of the hydro-meteorological events. Nevertheless, the downstream Bettollelle (BET) hydrometer kept working and measured more than 6 m of height flow. On the other hand, the Moie (MOI) and S. Severino (SSE) stations, which were respectively located in the basins of the Esino and Potenza rivers (Fig. 1), recorded lower flow heights, suggesting that the intensity of the hydro-meteorological event was reduced when moving southwards from Metauro and Misa.

Following an increasing usage of the seismic noise (i.e., also referred to as ‘ground vibration’) as monitoring tool for a broad spectrum of gravitational processes ranging from bedload transport to debris flows²¹, we computed the spectra of the seismic signals recorded at 54 stations spread over the area hit by the hydro-meteorological event (see Methods and Supplementary Figure 2). After some tests, we verified that the clearest imprinting of the flood event on the seismic signals appears in the frequency band 30–50 Hz, which shows peaks temporally particularly well correlated with the precipitation. For instance, the seismic signal acquired by the station ATPC, located at the Metauro river upstream, shows a remarkable temporal coincidence of its maxima with those of the surrounding rainguages (Fig. 2c). To better observe the temporal relationship among the different signals, we highlighted in Fig. 2c the signal of the seismic station ATPC. Similar indications are also provided by the SSFR station placed at the upstream of Esino River (Supplementary Fig. 3). Furthermore, we also compare the temporal evolution of data recorded by rainguages, hydrometer and seismic stations for both the Metauro and Misa rivers. It is worth to mention that the area between the two rivers has experienced the highest water level height and the larger damages. For each hydrometer associated to these two rivers, we plot the envelope of the two closest seismic stations and the data of the rainguages within 10 km from the seismic stations (Supplementary Figs. 4–7). Looking at these plots, it appears rather clear that the agreement between seismic data and rainfall amount is higher than that between seismic and water level data. This last evidence could also be due to the fact that our seismic stations are located a few kilometers away from the river (between 5.5 km and 12 km). Finally, it is worth to emphasize the characteristics of signals recorded by the station COR1, located at the Misa River downstream. This latter station, in fact, shows the largest power peaks in coincidence with the rainfall maximum registered by the rainguages (for instance, see the time series of the rain gauge named Barbara, highlighted in green in Fig. 2a) and before the flow height peaks registered by hydrometer station located in the lower part of the Misa basin, BET, (Fig. 2b). We hypothesize that the latter behavior is due to the large distance between the COR1 station and the Misa River (around 14 km), which could have prevented the detection of the seismic vibrations directly induced by the river flow at this station.

To quantify the qualitative agreement observed in the trend of the seismic and raingauge time series, we calculate the correlation coefficient between the cumulated seismic data at each station and the cumulated rainfall rate at the nearest raingauge (Figs. 3a–d). The correlation coefficients are shown in Fig. 3e as function of the distance between seismic and raingauge stations. The size of the marker scales with the value of the total rainfall cumulated during the whole precipitation event. Figure 3e shows for a large number of stations a correlation larger than 0.8 when the distances from rainguages are smaller than 4 km. At larger distances, we observe a slight overall decreasing trend of the correlation with the distance.

Further complementary information can be obtained by the spectrogram of signals recorded at ATPC seismic station (Fig. 4). The latter shows a first peak starting approximately at 8:00 a.m. of the 15 September, with this latter lasting almost 1 h. Then a second peak with high signal power occurred at 12:00 a.m. of the same day and lasted several hours. Both peaks cover a wide frequency range, with the largest values observed in the frequency band 30–50 Hz. Furthermore, also in this case, we compare the seismic signal with the temporal evolution of signals from rainguages located within 10 km from the seismic station. Interestingly, the temporal limits of the second maximum at ATPC well match those of the hourly cumulated rainfall registered at San Benedetto Vecchio and Monte Nerone rainguages. Hence, these results indicate that the seismic data will track the

duration of the precipitation event (between 12:00 and 20:00 UTC on the 15 September 2022), suggesting that the seismic stations captured the effects of the meteorological event.

Spatial coherence of seismic noise over time

We extended the analysis of the seismic signals looking at their spatial coherence over the areal extension of the 15 September flood event along the duration of the crisis. We compared the temporal evolution of the median seismic amplitude for the 54 considered stations (Fig. 4a and Supplementary Figs. 8–61). When we look at the average of the median amplitudes over all the stations (Fig. 5a, where amplitudes are represented in logarithmic scale), we observe two main features: (i) a 1-day periodicity and (ii) a peak in coincidence with the start of the precipitation event (i.e., around 12:00 am of the 15 September). While the one-day periodicity is a well-known kind of trend in seismic noise due to mainly anthropic sources²², the effects of rainfall on seismic amplitude is remarkable. Interestingly, the averaged seismic signal over the whole set of stations shows a marked increase starting from 12:00 am, which matches the time at which the measured rainfall and flow height start to sharply increase (see Fig. 2a, b and animation in the Supplemental Material). In Fig. 5a, we marked four timeframes (vertical dashed lines). Three of them correspond to frames before and after the hydro-meteorological event (black), while the fourth frame marks the strong rainfall phase. For each of these timeframes, we display the spatial coherency of seismic amplitudes (Fig. 5b–e, see “Methods” section). Before the onset and after the end of the high-rainfall phase (subpanels b, c, and e), we can observe that the largest seismic amplitudes show high coherency close to the seacoast, likely as an effect of the sea waves hitting the coast and producing coherent seismic noise (i.e., at periods around 5 s the seismic noise is referred as microseismic noise). Noteworthy, differently from all the others, subpanel 4d (representing the spatial distribution of seismic amplitudes during the rainfall crisis on 15 September at 5.50 pm), shows a large peak elongated in the south-west to north-east direction. The large seismic anomaly spatially well coincides with the basin between the Metauro and Misa rivers (blue lines), where indeed most damaged villages are located (black stars). Hereinafter, we discuss a possible interpretation of these results and their implications for the monitoring of hydro-meteorological events.

Discussion

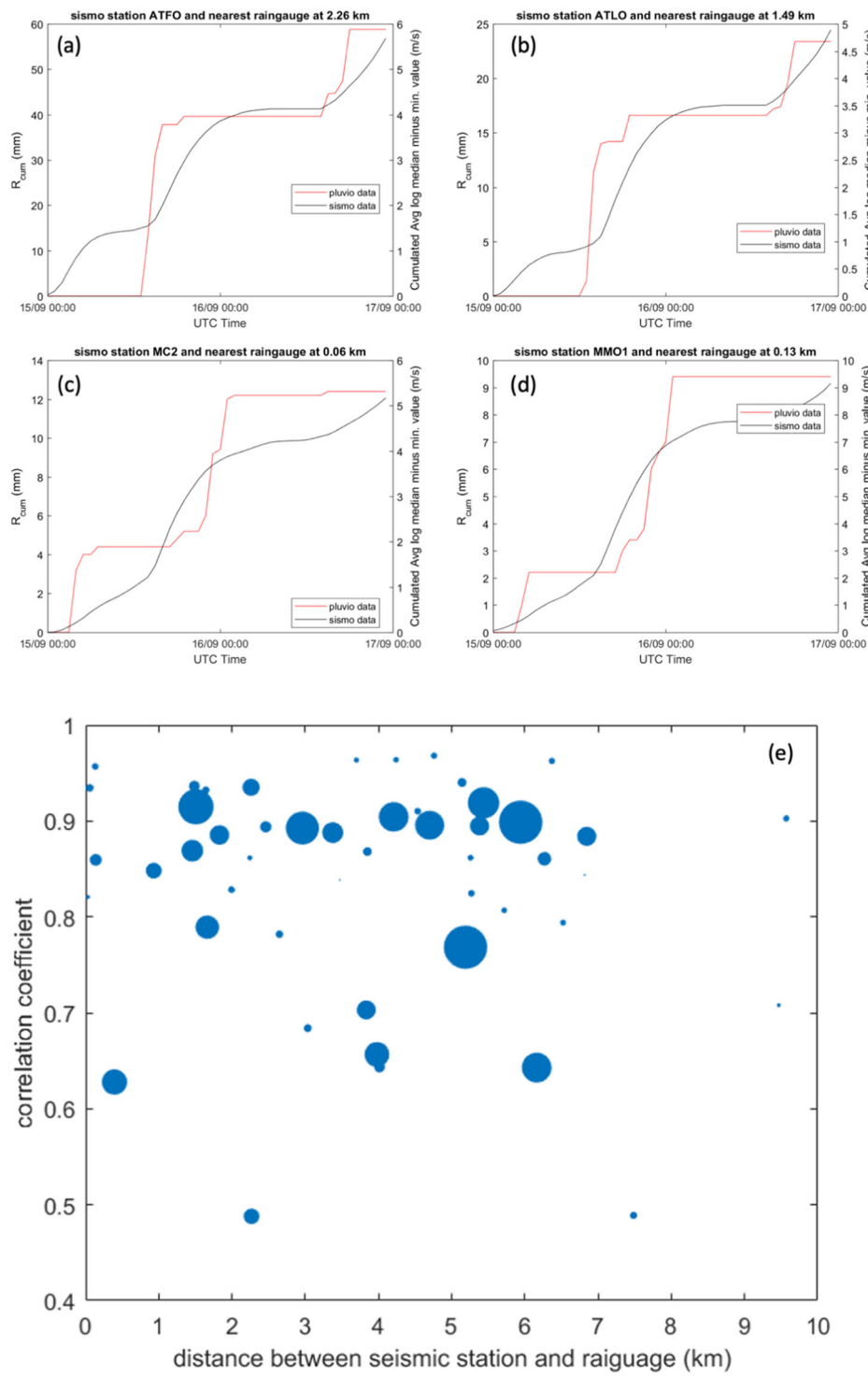
The rising trend of fatal flash floods occurrence recorded worldwide is probably the result of concomitant effects, such as the changes in environmental and global climatic settings²³, and the increases in population in areas that are at risk for flash floods.

Under this increasing risk for communities and infrastructures, additional research efforts are needed to better understand predisposing factors to nowcast the occurrence of critical events, as well as to develop reliable rapid responses to mitigate the exposure of people to risk.

In this work, we have studied the characteristics and spatio-temporal evolution of ground vibrations associated to large precipitation events by extracting and analyzing segments of continuous data of the stations of the Italian national seismic network downloaded from the ORFEUS-EIDA repository (<https://www.orfeus-eu.org/data/eida/>), where they are identified with the network code IV.

Although we have applied rather simple signal processing (time-frequency and spatial analyses of seismic signals), our results highlight that seismic noise observed at dense networks provides useful information concerning the flash floods upland catchments²¹. The adoption of approaches using ground vibration data analyses as monitoring tools for debris flows is increasing worldwide^{24–26}. Seismic records can be also used to retrieve rainfall, although to date only very few studies have investigated this possibility^{27,28}. Furthermore, recently¹⁰ it was shown that seismic approaches can also sense rapid flooding and provide information on flood magnitude, velocity and trajectory in near real-time. While these approaches from literature exploited mostly single or a few seismic sensors placed nearby the monitored rivers (Table 1), our work explored the possibility to characterize

Fig. 3 | Correlation coefficients as function of the seismometer-raingauge distance. a–d show examples of the comparison between the cumulated seismic amplitudes (black line) and the cumulated rainfall (red line) collected by the nearest raingauge. e Correlation coefficients computed between the cumulated seismic data and the cumulated rainfall as function of the distance between seismic station and the nearest raingauge. The size of the markers scales as the rainfall cumulated along the whole duration of the precipitation event (in mm).

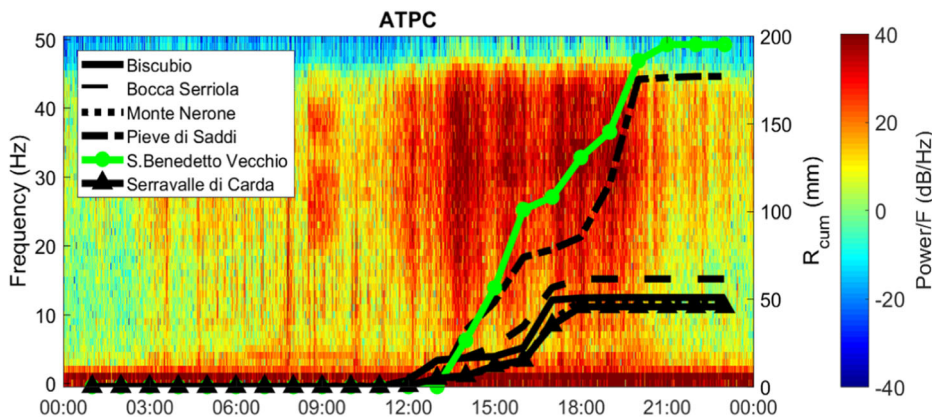


the seismic noise evolution in time and space when it is observed through seismic networks. A similar approach has been recently proposed by Diaz et al.²⁹, in which two rainfall episodes in the Eastern Pyrenees were identified during a temporary survey in the seismic signals of 140 high-frequency seismometers. Like in our approach, the authors successfully detected the progress of the precipitation by mapping the amplitude of the seismic noise over the dense (mean spacing 1.5 km) seismic network. However, in this case, the availability of the seismic network was limited to the duration of the experiment (April–June 2021). On the contrary, our study is based on the usage of the permanent Italian seismic monitoring network, which implies that the proposed approach could be in principle included in the workflow

of a real-time monitoring system for precipitation and debris flows. Furthermore, in our study, we also consider the water level data obtained by the hydrometers available in the area.

Cook et al.³⁰ used the 76 broadband stations of the permanent Uttarakhand seismic network (mean interstation spacing of 18.9 Km) to track the front propagation of the Dhauliganga flood event in Uttarakhand (northern India) integrated by data from 3 disdrometers and images from satellites and video cameras. Differently from our work, this study relied on array technique based on the cross-correlation among the traces and the spatial amplitude decay to localize the flood front.

Fig. 4 | Seismic noise temporal evolution. Spectrogram of the ATPC seismic station (Metauro upstream) on 15 September 2022. Black lines represent the hourly cumulated rainfall measured by the raingauges within 10 km from ATPC (please note that the names of the raingauges are listed in the legend and are highlighted in Fig. S1 of the Supplemental Material). The green line displays the hourly cumulated rainfall of the closest raingauge (i.e., 5.4 km away from ATPC).



Although array approaches might precisely track the front propagation, it is worth noting that they also present pitfalls. For instance, they properly work for very large phenomena, while for moderate or small events they can result in instability of the numerical solutions. With respect to this last issue, Cook et al.³⁰ could track the flow events even at stations 100 km far away from the source and take advantage of the seismic network for location, but for less intense events the detection would have been challenging. In that sense, we believe that array techniques are less robust for near real-time applications than a spatial interpolation of single-station amplitude and spectral properties of the seismic noise.

While, as discussed, a few attempts of detecting catastrophic flow events with regional seismic networks exist, it is worth noting that none of them has used permanent seismic, hydrometric and raingauge stations with comparable density of the networks adopted in our study. Our results suggest that the setup considered in our work combined with simple single-station numerical analysis spatially integrated over the networks could provide a powerful tool to settle a permanent multi-parameter real-time monitoring system.

It is worth noting that upscaling the signal strategies from data recorded at short distances from small rivers confined in valleys to large scale events is challenging. This is indeed the case of the Marche flood crisis of the 15 and 16 September 2022, which affected an area of 550 km². Nevertheless, the scientific community is increasingly engaged in this research field with the aim to opportunistically complement data from existing networks (e.g., raingauges, disdrometers, hydrometers), which might suffer of insufficient density, low sampling rate, saturation, and large latency, with other pieces of information.

We have shown that during the most intense part of the Marche precipitation event (i.e., from 12:00 to 20:00 UTC of the 15 September 2022) the seismic power in the frequency band 30–50 Hz significantly increases and presents remarkable temporal coincidence with maxima at raingauge recordings. Therefore, seismic noise amplitudes during this stage of the event are likely related to the rainfall intensity and size of the meteorological event. These latter are pieces of information that seismic networks can provide in real-time and with high sampling rate and thus could easily complement classic real-time monitoring systems, ground-based weather radars, and satellite-borne active and passive sensors.

Furthermore, by following the spatio-temporal evolution of signal amplitudes recorded by seismic stations in the region, we have shown that seismic noise also provides useful information to track the evolution of the precipitation and flooding event. Indeed, the region with higher seismic amplitudes matches the area between the Metauro and Misa rivers, which hosted severely damaged villages. Notably the anomalous high amplitudes of seismic data anticipate by a few hours the major flooding, thus suggesting that the seismic noise amplitudes are related to both the rainfall intensity and the increasing discharge in the basin headwaters. Our results highlight a stronger correlation between the seismic noise amplitudes and the intensity of the precipitation than the correlation between the former and

hydrometric data. However, the location of the seismic stations with respect to the rivers can have influenced these results. It is an established fact that seismic noise depends on various factors²².

Following the idea of exploiting the seismic noise for monitoring hydro-meteorological events, future studies should hence investigate how to assess the contribution of different and combined sources (e.g., rainfall, wind, and increasing discharge in the basin headwaters) to its temporal and spatial evolution. If it were possible to discriminate and to characterize in real-time the contribution of the different processes to seismic noise, then we would be in the condition to integrate these pieces of information within well-established procedures to early detect the occurrence of flash floods at regional scale. With respect to such a goal, our study represents the first step of a long journey.

Following the pioneering study of 2012 by Tsai and colleagues³¹, who provided an analytical model for seismic noise produced by impacting river sediments, a priority step is certainly the definition of novel analytical models that would combine both the contribution described by Tsai and colleagues and the effect of rainfall intensity on seismic noise. However, to provide an empirical relation between rainfall rate and seismic noise amplitude, data from co-located disdrometer and seismic station are needed. With respect to raingauges, disdrometers provide much richer information on precipitation characteristics and they will allow to better interpret seismic noise. Being able to provide information about the intensity of precipitation from seismic data can lead to a better accuracy of streamflow simulation and flood forecasting³².

A further target is to extend the approach proposed by Dietze and colleagues¹⁰ to large scale monitoring networks to obtain real-time estimation of flood volume, velocity, and trajectory. With respect to the latter goal, both the study of processes contributing to the generation of seismic noise, the definition of regional scale models describing the attenuation of seismic signals generated by floods with distance and the required network density for the detection and characterization of flood events in seismic noise would be relevant. In this regard, an important step would also be to collect and organize datasets combining multiparametric signals related to large flood events that occurred in recent years. The creation of catalogs of well-recorded large-scale flood episodes would foster the cooperation among seismologists and hydrologists and would likely lead to improved approaches for the real-time detection and characterization of future catastrophic floods.

Methods

Seismic data

We selected continuous data in the period 13.09.202–17.09.2022 from three-component seismic stations located in the latitude-longitude ranges 42.7–44.350 and 11.9–13.9, respectively. Recordings of 54 seismic stations from the Italian national seismic network³⁰ (network code IV) in this time interval have been downloaded from the ORFEUS-EIDA repository (<https://www.orfeus-eu.org/data/eida/>) and processed. Continuous signals

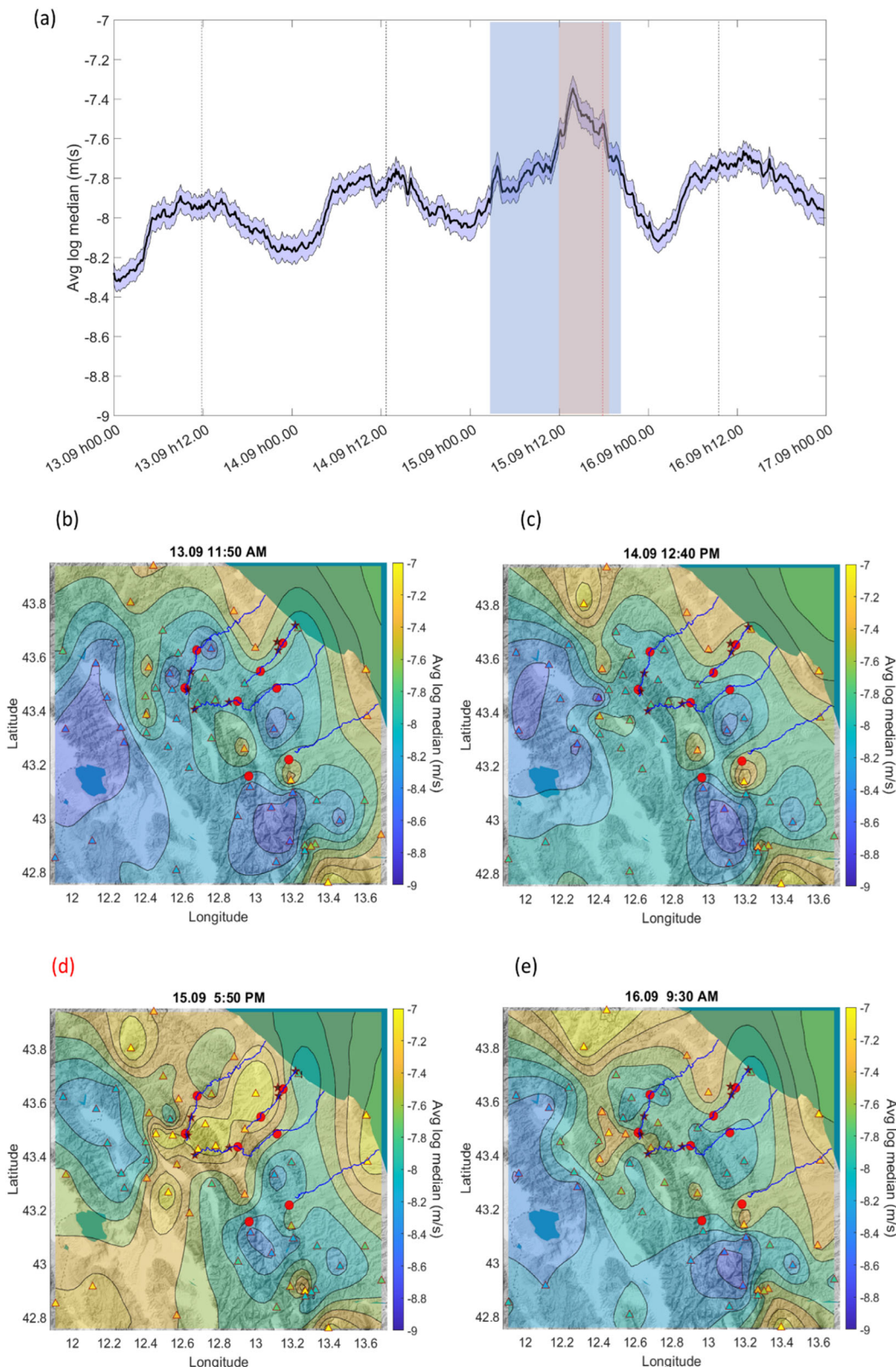


Fig. 5 | Spatial coherence of seismic noise over time. **a** Time history of the median amplitude of the seismic signal averaged over the stations and corresponding standard deviation (log scale). The vertical dotted lines mark the time frames at which the spatial distribution of the seismic amplitude is displayed in the following subpanels. The blue and brown shaded areas broadly mark respectively the time interval with intense rain and with the largest seismic amplitude. **b–e** Spatial distribution of the amplitude of the seismic signals (hf, z component) at four

timeframes. Triangles mark the station positions and colors scale with the signal amplitude (in m/s - log scale). Isolines display the amplitude of the seismic signal interpolated over the whole target area (see methods for details). Red circles show the position of hydrometers, while black stars are located at the position of strongly damaged villages or towns. The four blue irregular lines show the rivers (from north to south) Metauro, Misa, Esino, Potenza.

have been frequency filtered in the bands 0.5–2 Hz and 30–50 Hz, labeled respectively as low-frequency (lf) and high-frequency (hf) bands. Envelopes on the signals in the two frequency bands have been computed and then downsampled at one sample per minute. The median of the detrended envelopes at each seismic station was then calculated in a time window of 15 min sliding 10 min at each step. Finally, amplitudes of the seismic envelopes have been spatially interpolated using the model³³ $\frac{x}{D} - \left(\frac{x}{D}\right)^3$, where x is the distance between sampled and interpolated point and D defines the interpolation range and was fixed to 1 degree.

Hydro-meteorological data

For the same period and area considered for seismic data, we downloaded data from 270 raingauges managed by Regione Marche and Regione Umbria. The data consists of time series of rainfall amount (in mm) collected in a given time interval, which can vary between 15 min and 60 min. All data have been cumulated over 60 min to obtain the hourly cumulated rainfall.

The hydrometer data used in the work are managed by Regione Marche and consists of the measurement of the water level (in m) at the station each 30 min.

Data availability

We used seismic data from the networks IV (INGV Seismological Data Centre, 2006³⁴), which are available via the website: <https://www.orfeus-eu.org/data/eida/>. Hydro-meteorological data are available at <http://app.protezionecivile.marche.it/sol/indexjs.sol?lang=it> for the hydrometers and raingauges managed by Regione Marche and at <https://www.regione.umbria.it/-/servizio-idografico> for the raingauges managed by Umbria Region. The data are freely available upon registration for Regione Marche and upon request for Regione Umbria.

Code availability

Data was processed and all figures were created using MATLAB R2019b (<https://www.mathworks.com/products/matlab.html>). For inquiries about the code please contact matteo.picozzi@unina.it or mauro.palo@unina.it.

Received: 11 October 2023; Accepted: 26 April 2024;

Published online: 01 August 2024

References

1. Gaume, E. et al. A compilation of data on European flash floods. *J. Hydrol.* **367**, 70–78 (2009).
2. Amponsah, W. et al. Integrated high-resolution dataset of high-intensity European and Mediterranean flash floods. *Earth Syst. Sci. Data* **10**, 1783–1794 (2018).
3. Bates, P. D. et al. A climate-conditioned catastrophe risk model for UK flooding. *Nat. Hazards Earth Syst. Sci.* **23**, 891–908 (2023).
4. Tramblay, Y. & Somot, S. Future evolution of extreme precipitation in the Mediterranean. *Clim. Change* **151**, 289–302 (2018).
5. Cassola, F., Iengo, A., & Turato, B. (2023). Extreme convective precipitation in Liguria (Italy): a brief description and analysis of the event occurred on October 4, 2021. *Bull. Atmos. Sci. Technol.* **4**, 4 (2023).
6. Santo, A., Di Crescenzo, G., Del Prete, S. & Di Iorio, L. The Ischia island flash flood of November 2009 (Italy): phenomenon analysis and flood hazard. *Phys. Chem. Earth, Parts A/B/C* **49**, 3–17 (2012).
7. Pulvirenti, L., Squicciarino, G., Fiori, E., Candela, L. & Puca, S. Analysis and processing of the COSMO-SkyMed second generation images of the 2022 marche (Central Italy) flood. *Water* **15**, 1353.13 (2023).
8. Kidd, C. et al. So, how much of the Earth's surface is covered by rain gauges? *Bull. Amer. Meteorol. Soc.* **98**, 69–78 (2017).
9. Sebastianelli, S., Russo, F., Napolitano, F. & Baldini, L. On precipitation measurements collected by a weather radar and a rain gauge network. *Nat. Hazards Earth Syst. Sci.* **3**, 605, <https://doi.org/10.5194/nhess-13-605-2013> (2013).
10. Dietze, M., Hoffmann, T., Bell, R., Schrott, L. & Hovius, N. A seismic approach to flood detection and characterization in upland catchments. *Geophys. Res. Lett.* **49**, e2022GL100170 (2022).
11. Borga, M., Stoffel, M., Marchi, L., Marra, F. & Jakob, M. Hydrogeomorphic response to extreme rainfall in headwater systems: flash floods and debris flows. *J. Hydrol.* **518**, 194–205 (2014).
12. Chmiel, M. et al. Brief communication: seismological analysis of flood dynamics and hydrologically triggered earthquake swarms associated with Storm Alex. *Nat. Hazards Earth Syst. Sci.* **22**, 1541–1558 (2022).
13. Smith, K. & Tape, C. Seismic Noise in Central Alaska and influences from rivers, wind, and sedimentary basins. *J. Geophys. Res. Solid Earth* **124**, 11678–11704 (2019).
14. Govi, M., Maraga, F. & Moia, F. Seismic detectors for continuous bed load monitoring in a gravel stream. *Hydrol. Sci.* **38**, 123–132 (1993).
15. Burtin, A., Bollinger, L., Vergne, J., Cattin, R. & Nábělek, J. L. Spectral analysis of seismic noise induced by rivers: a new tool to monitor spatiotemporal changes in stream hydrodynamics. *J. Geophys. Res.* **113**, B05301 (2008).
16. Hsu, L., Finnegan, N. J. & Brodsky, E. E. A seismic signature of river bedload transport during storm events. *Geophys. Res. Lett.* **38**, 1–6 (2011).
17. Schmandt, B., Aster, R. C., Scherler, D., Tsai, V. C. & Karlstrom, K. Multiple fluvial processes detected by riverside seismic and infrasound monitoring of a controlled flood in the Grand Canyon. *Geophys. Res. Lett.* **40**, 4858–4863 (2013).
18. Burtin, A., Hovius, N. & Turowski, J. M. Seismic monitoring of torrential and fluvial processes. *Earth Surf. Dynam.* **4**, 285–307 (2016).
19. Borga, M. et al. Integrated post-event survey of the record-breaking Central Italy flash flood of September 2022: observation strategy and lessons learned. in *EGU General Assembly 2023*. p. 16248 (2023).
20. Fiorucci, F. et al. Characteristics of the landslides triggered by the extraordinary rainfall event occurred in Central Italy on September 15, 2022. in *EGU General Assembly 2023*. p. 7184 (2023).
21. Coviello, V., Arattano, M., Comiti, F., Macconi, P. & Marchi, L. Seismic characterization of debris flows: Insights into energy radiation and implications for warning. *J. Geophys. Res.: Earth Surf.* **124**, 1440–1463 (2019).
22. Gutenberg, B. Microseisms. *Advan. Geophys.* **5**, 53–92 (1958).
23. Tabari, H. Climate change impact on flood and extreme precipitation increases with water availability. *Sci. Rep.* **10**, 13768 (2020).
24. Abancó, C., Hürlimann, M. & Moya, J. Analysis of the ground vibration generated by debris flows and other torrential processes at the Rebaixader monitoring site (Central Pyrenees, Spain). *Nat. Hazards Earth Syst. Sci. Discuss.* **14**, 929–943 (2014).
25. Coviello, V., Arattano, M. & Turconi, L. Detecting torrential processes from a distance with a seismic monitoring network. *Nat. Hazards* **78**, 2055–2080 (2015).
26. Walter, F. et al. Testing seismic amplitude source location for fast debris-flow detection at Illgraben, Switzerland. *Nat. Hazards Earth Syst. Sci.* **17**, 939–955 (2017).
27. Bakker, M. et al. Seismic modelling and observations of rainfall. *J. Hydrol.* **610**, 127812 (2022).
28. Rindraharisaona, E. J. et al. Seismic signature of rain and wind inferred from seismic data. *Earth Space Sci.* **9**, e2022EA002328 (2022).
29. Diaz, J. et al. Monitoring storm evolution using a high-density seismic network. *Sci. Rep.* **13**, 1853 (2023).
30. Cook, K. L. et al. Detection and potential early warning of catastrophic flow events with regional seismic networks. *Science* **374**, 87–92 (2021).
31. Tsai, V. C., Minchew, B., Lamb, M. P. & Ampuero, J.-P. A physical model for seismic noise generation from sediment transport in rivers. *Geophys. Res. Lett.* **39**, L02404 (2012).
32. Borga, M. Accuracy of radar rainfall estimates for streamflow simulation. *J. Hydrol.* **267**, 26–39 (2002).

33. jBuist. *MATLAB Central File Exchange*. <https://it.mathworks.com/matlabcentral/fileexchange/57133-kriging-x-y-z-range-sill> (2023).
34. INGV Seismological Data Centre. *Rete sismica nazionale (RSN), Istituto Nazionale di Geofisica e Vulcanologia (INGV)*. (2006).

Acknowledgements

Dedicated to Velio, colleague but above all friend who we miss dearly every day but who will always accompany us for his enthusiasm, human warmth and scientific vision. Figures were done using Matlab software (R2019b, <https://it.mathworks.com/>, last accessed December 2023).

Author contributions

V.C. conceived the work and prepared the datasets. All authors jointly analyzed the data, interpreted the results, and wrote the manuscript.

Competing interests

The authors declare no competing interests.

Additional information

Supplementary information The online version contains supplementary material available at <https://doi.org/10.1038/s44304-024-00018-7>.

Correspondence and requests for materials should be addressed to Matteo Picozzi.

Reprints and permissions information is available at <http://www.nature.com/reprints>

Publisher's note Springer Nature remains neutral with regard to jurisdictional claims in published maps and institutional affiliations.

Open Access This article is licensed under a Creative Commons Attribution 4.0 International License, which permits use, sharing, adaptation, distribution and reproduction in any medium or format, as long as you give appropriate credit to the original author(s) and the source, provide a link to the Creative Commons licence, and indicate if changes were made. The images or other third party material in this article are included in the article's Creative Commons licence, unless indicated otherwise in a credit line to the material. If material is not included in the article's Creative Commons licence and your intended use is not permitted by statutory regulation or exceeds the permitted use, you will need to obtain permission directly from the copyright holder. To view a copy of this licence, visit <http://creativecommons.org/licenses/by/4.0/>.

© The Author(s) 2024